



Thermodynamics of deformed AdS-Schwarzschild black hole

Mohammad Reza Khosravipoor^a, Mehrdad Farhoudi^b 

Department of Physics, Shahid Beheshti University, Evin, Tehran 19839, Iran

Received: 8 September 2023 / Accepted: 4 November 2023 / Published online: 16 November 2023
© The Author(s) 2023

Abstract By implementing the gravitational decoupling method, we find the deformed AdS-Schwarzschild black hole solution when there is also an additional gravitational source, which obeys the weak energy condition. We also deliberately choose its energy density to be a certain monotonic function consistent with the constraints. In the method, there is a positive parameter that can adjust the strength of the effects of the geometric deformations on the background geometry, which we refer to as a deformation parameter. The condition of having an event horizon limits the value of the deformation parameter to an upper bound. After deriving various thermodynamic quantities as a function of the event horizon radius, we mostly focus on the effects of the deformation parameter on the horizon structure, the thermodynamics of the solution and the temperature of the Hawking–Page phase transition. The results show that with the increase of the deformation parameter: the minimum horizon radius required for a black hole to have local thermodynamic equilibrium and the minimum temperature below which there is no black hole decrease, and the horizon radius of the phase transition and the temperature of the first-order Hawking–Page phase transition increase. Furthermore, when the deformation parameter vanishes, the obtained thermodynamic behavior of the black hole is consistent with that stated in the literature.

1 Introduction

Before the 1970s, there was no compelling reason to study the thermodynamics of black holes, until Hawking’s area theorem changed this view [1]. Then, Bekenstein linked Hawking’s area theorem with the second law of thermodynamics by assigning entropy to black holes [2]. Using such similarity and assuming the event horizon of black holes as a Killing

horizon, the four laws of black hole mechanics were formulated [3]. However, with the classical view that black holes absorb all matter and energy and emit no radiation, attributing temperature and entropy to black holes was questionable. But by using quantum effects, Hawking showed that black holes have radiation with the spectrum of a black body with a certain temperature [4]. After the formulation of the standard laws of thermodynamics of black holes, several interpretations and investigations were carried out in the thermodynamics committee about black holes, such as entropy and temperature, the first law of thermodynamics, and relations between extensive and intensive quantities, see, e.g., Refs. [5,6] and references therein.

The thermodynamic laws of ordinary materials are associated with a pressure-volume term, however those for black holes do not contain such a term. To overcome this inconsistency, an idea based on the immersion of black holes in a background with a negative cosmological constant was presented [7]. In this view, pressure can be considered equal to a negative cosmological constant. In this regard, in the context of black hole thermodynamics, black holes with asymptotic anti-de Sitter (AdS) are more interesting. The idea of using the cosmological constant as the thermodynamic pressure [8,9] generalized the first law of black hole thermodynamics and formed an extended phase-space, see, e.g., Refs. [10,11]. Hence, in the presence of the cosmological constant, the mass of a black hole does not represent the internal energy of the thermodynamic system and is interpreted as the gravitational version of the enthalpy [12].

The new perspective of black hole thermodynamics based on the new interpretation of the cosmological constant and black hole mass has led to new phenomena associated with black holes. Accordingly, topics such as thermodynamic equilibrium and phase transition can be addressed. One of the most important thermodynamic behaviors is the phase transition between sufficiently large (compared to the AdS radius) black holes and an environment full

^a e-mail: m_khosravipoor@sbu.ac.ir

^b e-mail: m-farhoudi@sbu.ac.ir (corresponding author)

of special radiation. This is known as the Hawking–Page phase transition [13], which is considered as a confinement/deconfinement phase transition in boundary conformal field theory [14].

Furthermore, black hole thermodynamics has wide range of applications compared to the Einstein gravity. Even, the investigation of more complex behaviors in the issue of the thermodynamic phase transition of black holes in modified gravitational theories has received much attention, see, e.g., Refs. [15, 16]. In general, finding a black hole as a solution in a gravitational theory leads to the investigation of thermodynamic behavior from the researchers' point of view. Subsequently, more studies have been conducted and other novel phenomena and phase structures have been observed, see, e.g., Refs. [17–22].

The non-linear nature of equations in gravitational theories leads to approximate methods and, of course, innovative proposals for finding analytical solutions, which is always an important task. In this regard, one of the attractive approach for searching and analyzing solutions of the gravitational equations is the gravitational decoupling (GD) method, which serves as a useful tool, see, e.g., Refs. [23–25] and references therein. Through this method, the known solutions of the standard gravitational action can be extended (with some minimal set of requirements) to additional sources and the domain of modified gravitational theories. The implementation of the GD method makes it possible to decouple the gravitational equations of sources into two parts, one for the standard field equations and one for an additional gravitational source. This method has been applied in the context of the Randall-Sundrum brane-world [26, 27] and has also been extended to investigate in other gravitational issues, including new black hole solutions, see, e.g., Refs. [25, 28–40]. In the present work, while employing the GD method, we intend to extend the AdS-Schwarzschild vacuum solution in the presence of a generic gravitational source, which satisfies the weak energy condition. Thereafter, we try to find possible deformed AdS-Schwarzschild black hole solution and then investigate its thermodynamic properties and Hawking–Page phase transition while varying the relevant parameters.

The work is organized as follows. In Sect. 2, while briefly reviewing and implementing the GD method, we introduce the desired gravitational action. In Sect. 3, we derive the deformed AdS-Schwarzschild black hole. In Sect. 4, we scrutinize the structure of the horizon and calculate the thermodynamic quantities in the extended phase-space to investigate the horizon structure, the thermodynamics of the solution and the temperature of the Hawking–Page phase transition. Finally, we summarize the results in Sect. 5.

2 Modified gravitational action and decoupling field equations

We consider the following action in four dimensions in which an additional general Lagrangian term is added to the standard Einstein gravity with the cosmological constant, namely

$$A = \int d^4x \sqrt{-g} \left(\frac{R - 2\Lambda}{2\kappa} + L_m + L_X \right), \quad (1)$$

where g is the determinant of the metric, R is the Ricci scalar, Λ is the cosmological constant, L_m is the usual matter Lagrangian and L_X represents Lagrangian for any other matter or new gravitational sector beyond general relativity, e.g. Lovelock gravity and/or new other scalar/vector/tensor field(s). Meanwhile, $\kappa = 8\pi G_N/c^4$, however through the work, we use the natural units $\hbar = 1 = c$, and also employ the $(-, +, +, +)$ signature. The variation of the action with respect to the metric gives the field equations

$$G_{\mu\nu} + \Lambda g_{\mu\nu} = \kappa T_{\mu\nu}^{(\text{tot})}, \quad (2)$$

where $G_{\mu\nu}$ is the Einstein tensor and $T_{\mu\nu}^{(\text{tot})}$ represents the total symmetric energy–momentum tensor as

$$T_{\mu\nu}^{(\text{tot})} = T_{\mu\nu}^{(m)} + T_{\mu\nu}^{(X)}, \quad (3)$$

wherein

$$T_{\mu\nu}^{(m)} = -\frac{2}{\sqrt{-g}} \frac{\delta(\sqrt{-g} L_m)}{\delta g^{\mu\nu}} \quad (4)$$

and

$$T_{\mu\nu}^{(X)} = -\frac{2}{\sqrt{-g}} \frac{\delta(\sqrt{-g} L_X)}{\delta g^{\mu\nu}}. \quad (5)$$

As an ansatz, we demand the solution to be the spherically symmetric and static spacetime, namely

$$ds^2 = -e^{\nu(r)} dt^2 + e^{\mu(r)} dr^2 + r^2(d\theta^2 + \sin^2\theta d\phi^2), \quad (6)$$

in the spherical coordinates. Hence, metric (6) must satisfy the field Eq. (2), namely

$$\kappa \left(T_{00}^{(m)0} + T_{00}^{(X)0} \right) = \Lambda + e^{-\mu} \left(\frac{1}{r^2} - \frac{\mu'}{r} \right) - \frac{1}{r^2}, \quad (7)$$

$$\kappa \left(T_{11}^{(m)1} + T_{11}^{(X)1} \right) = \Lambda + e^{-\mu} \left(\frac{1}{r^2} + \frac{\nu'}{r} \right) - \frac{1}{r^2}, \quad (8)$$

$$\kappa \left(T_{22}^{(m)2} + T_{22}^{(X)2} \right) = \Lambda + \frac{1}{4} e^{-\mu} \left[-\mu' \nu' + 2\nu'' + \nu'^2 + \frac{2(\nu' - \mu')}{r} \right], \quad (9)$$

where prime denotes derivative with respect to r and $T_{33}^{(\text{tot})3} = T_{22}^{(\text{tot})2}$ due to the spherical symmetry. However, we effectively identify the energy–momentum tensors as

$$T_{\mu}^{(\text{tot})\nu} = \text{diag}[-\tilde{\epsilon}, \tilde{p}_r, \tilde{p}_t, \tilde{p}_t], \quad (10)$$

$$T_{\mu}^{(m)\nu} = \text{diag}[-\epsilon, p_r, p_t, p_t], \quad (11)$$

$$T^{(X)}_{\mu\nu} = \text{diag}[-\mathcal{E}, \mathcal{P}_r, \mathcal{P}_t, \mathcal{P}_t], \tag{12}$$

where $(\tilde{\epsilon}, \epsilon$ and $\mathcal{E})$ are energy densities, $(\tilde{p}_r, p_r$ and $\mathcal{P}_r)$ are radial pressure densities, and $(\tilde{p}_t, p_t$ and $\mathcal{P}_t)$ are tangential pressure densities. In general, when $\tilde{p}_t \neq \tilde{p}_r$, these definitions clearly indicate an anisotropy case.

In addition, the conservation equation

$$\nabla_\mu T^{(\text{tot})\mu\nu} = 0, \tag{13}$$

with metric (6), is a linear combination of Eqs. (7)–(9). However, in terms of those two sources in relation (3), while using relations (10)–(12), it gives

$$\begin{aligned} \frac{2}{r}(p_r - p_t + \mathcal{P}_r - \mathcal{P}_t) + \frac{v'}{2}(\epsilon + p_r + \mathcal{E} + \mathcal{P}_r) \\ + (p'_r + \mathcal{P}'_r) = 0. \end{aligned} \tag{14}$$

Now, to solve the system Eqs. (7)–(9), we implement the GD method, which is explained in detail in Ref. [24], of course, we mention the necessary steps very briefly. We assume that the solution of Eqs. (7)–(9) for the source $T^{(m)}_{\mu\nu}$ when $T^{(X)}_{\mu\nu} = 0$ is a general static spherically symmetric one as

$$ds^2|_{T^{(X)}_{\mu\nu}=0} = -e^{\zeta(r)} dt^2 + e^{\lambda(r)} dr^2 + r^2(d\theta^2 + \sin^2\theta d\phi^2). \tag{15}$$

The energy–momentum tensor $T^{(m)}_{\mu\nu}$ is conserved with this metric, i.e.

$$\tilde{\nabla}_\mu T^{(m)\mu\nu} = 0, \tag{16}$$

where $\tilde{\nabla}_\mu$ is calculated according to metric (15). We also assume that the effects of the presence of the source $T^{(X)}_{\mu\nu}$ on solution (15) are in the geometric deformation

$$\zeta \rightarrow v = \zeta + \alpha g(r) \tag{17}$$

and

$$e^{-\lambda} \rightarrow e^{-\mu} = e^{-\lambda} + \alpha f(r), \tag{18}$$

where $f(r)$ and $g(r)$ are geometric deformations that alter the radial and temporal metric components, respectively, and the constant α is a free positive parameter, which can somehow adjust the strength of the effects on these components simultaneously. Moreover, having α guarantees that solution (15) is recovered in the limit $\alpha \rightarrow 0$. We refer to the parameter α as a deformation parameter.

Then, substituting decompositions (17) and (18) into the original field Eqs. (7)–(9) causes those to be separated into two decoupled sets of equations. One set of the field equations is for the standard energy–momentum tensor $T^{(m)}_{\mu\nu}$, i.e.

$$\kappa \epsilon = -\Lambda - e^{-\lambda} \left(\frac{1}{r^2} - \frac{\lambda'}{r} \right) + \frac{1}{r^2}, \tag{19}$$

$$\kappa p_r = \Lambda + e^{-\lambda} \left(\frac{1}{r^2} + \frac{\zeta'}{r} \right) - \frac{1}{r^2}, \tag{20}$$

$$\kappa p_t = \Lambda + \frac{1}{4} e^{-\lambda} \left[-\lambda' \zeta' + 2\zeta'' + \zeta'^2 + \frac{2(\zeta' - \lambda')}{r} \right]. \tag{21}$$

Another set of the field equations is for the source $T^{(X)}_{\mu\nu}$, i.e.

$$\kappa \mathcal{E} = -\frac{\alpha f}{r^2} - \frac{\alpha f'}{r}, \tag{22}$$

$$\kappa \mathcal{P}_r - \alpha \frac{e^{-\lambda} g'}{r} = \alpha f \left(\frac{1}{r^2} + \frac{v'}{r} \right), \tag{23}$$

$$\begin{aligned} \kappa \mathcal{P}_t - \frac{\alpha e^{-\lambda}}{4} \left(2g'' + \alpha g'^2 + \frac{2g'}{r} + 2g'\zeta' - \lambda'g' \right) \\ = \frac{\alpha f}{4} \left(2v'' + v'^2 + 2\frac{v'}{r} \right) + \frac{\alpha f'}{4} \left(v' + \frac{2}{r} \right), \end{aligned} \tag{24}$$

which clearly shows that when the deformation parameter is zero, this source vanishes.

At this stage, one can investigate the field Eqs. (19)–(21) to determine $(T^{(m)}_{\mu\nu}, \zeta, \lambda)$, and then solve the field Eqs. (22)–(24) to specify $(T^{(X)}_{\mu\nu}, g, f)$. In other words, both sets, although separated, remain gravitationally connected, i.e. to solve the second set, one needs first to solve the first set. However, since the number of unknowns in each set of equations is more than the number of independent equations, it is necessary to apply additional conditions and/or extra relations, e.g. the equation of state. More explicitly, after solving the first set, five unknowns remain in the three equations corresponding to the additional source. Hence, to solve this set, we need to impose two constraints, which we will perform in the next section.

3 Deformation of AdS-Schwarzschild black hole

In order to deform AdS-Schwarzschild black hole for action (1), we start in the absence of L_X and with the solution of the exterior Schwarzschild (i.e., in vacuum with $T^{(m)}_{\mu\nu} = 0$) in the AdS background. In this regard, the field Eq. (2) give

$$e^{\zeta(r)}|_{T^{(m)}_{\mu\nu}=0} = e^{-\lambda(r)}|_{T^{(m)}_{\mu\nu}=0} = 1 - \frac{2M}{r} + \frac{r^2}{l^2} \tag{25}$$

for the region $r > R$, where R is the surface of the self-gravitating system, M is the ADM mass and $l = \sqrt{3/|\Lambda|}$ is the AdS radius.

In order to have black holes with a well-defined event horizon structure for action (1), the sufficient condition (i.e., the Kerr–Schild condition)

$$e^{\mu(r)} = e^{-\nu(r)} \tag{26}$$

can be imposed [25] on metric (6). Actually, by adding this ansatz, the deformed black hole metric is a metric that respects the symmetries. Accordingly, a direct consequence

of Eqs. (7) and (8) plus condition (26) is that the total source $T_{\mu\nu}^{(\text{tot})}$ must satisfy the equation of state

$$\tilde{p}_r = -\tilde{\epsilon}. \tag{27}$$

When $T_{\mu\nu}^{(m)} = 0$, this relation yields the constraint

$$[\mathcal{P}_r = -\mathcal{E}]|_{T_{\mu\nu}^{(m)}=0}, \tag{28}$$

i.e., in this case, with positive energy density of the source $T_{\mu\nu}^{(X)}$, only its negative radial pressure density is allowed. Furthermore, by deriving the conservation of the energy–momentum tensor of sources with metric (6) while using decompositions (17) and (18) as well as using relations (11) and (16), the first equality in relation (25), and condition (26), gives¹

$$\nabla_\mu T^{(m)\mu}_\nu = -\frac{\alpha g'}{2}(\epsilon + p_r)\delta_{1\nu} = -\nabla_\mu T^{(X)\mu}_\nu. \tag{29}$$

This relation, while assures the decoupling of the field equations, shows the exchange of energy between the sources. Moreover, from relation (29), it is obvious that there is no energy exchange in the absence of $T_{\mu\nu}^{(m)}$, or in the special case where $\epsilon = -p_r$, and/or when the geometric deformation g is constant.

From now on, for simplicity, we consider the background geometry to be the AdS-Schwarzschild vacuum, i.e. when $T_{\mu\nu}^{(m)} = 0$ and we have solution (25), but henceforth we do not mention the subscript. In fact, in the continuation, our aim is to explore the back-reaction of a static, spherically-symmetric energy–momentum tensor on the four-dimensional AdS-Schwarzschild black hole. Of course, it should be noted that in the mentioned case, one can get the solution without resorting to the GD method. However, we utilize the GD method as an alternative approach to solve this case to better observe the effect of moving away from the AdS-Schwarzschild solution and also to benefit from varying the deformation parameter when studying the thermodynamic properties. In other words, the merit of the GD method, in general, is that it is easy any interpretation in terms of energy exchange as well as in terms of superposition of configurations.

Accordingly, in the next step, by substituting condition (26) and the AdS-Schwarzschild solution (25) into decompositions (17) and (18), we obtain

$$\alpha f(r) = \left(1 - \frac{2M}{r} + \frac{r^2}{l^2}\right) [e^{\alpha g(r)} - 1]. \tag{30}$$

Hence, the line element (6) becomes

$$ds^2 = -e^{\xi(r)} B(r) dt^2 + \frac{1}{e^{\xi(r)} B(r)} dr^2$$

¹ It is instructive to emphasize that the use of the first equality in relation (25) and condition (26) is necessary to obtain the result of Eq. (29).

$$+r^2(d\theta^2 + \sin^2\theta d\phi^2), \tag{31}$$

where

$$B(r) \equiv e^{\alpha g(r)}. \tag{32}$$

Therefore, to completely specify the line element (6) in this case, we need to specify the behavior of function $B(r)$ (or indeed $g(r)$).

Now, using Eqs. (22) and (30), the differential equation governing the function $B(r)$ reads

$$r^2\kappa \mathcal{E} = \left(2M - r - \frac{r^3}{l^2}\right) B'(r) + \left(1 + \frac{3r^2}{l^2}\right) [1 - B(r)]. \tag{33}$$

Equation (33) shows that the behavior of function $B(r)$ depends on the function of energy density \mathcal{E} , which in turn depends on the choice of $T_{\mu\nu}^{(X)}$ as the additional source. To proceed, we resort to the weak energy condition for the $T_{\mu\nu}^{(X)}$, namely

$$\mathcal{E} \geq 0, \tag{34}$$

$$\mathcal{E} + \mathcal{P}_r \geq 0, \tag{35}$$

$$\mathcal{E} + \mathcal{P}_t \geq 0. \tag{36}$$

In the special case under consideration, due to constraint (28), condition (35) holds. Considering Eq. (33), condition (34) puts the constraint

$$\left(2M - r - \frac{r^3}{l^2}\right) B'(r) + \left(1 + \frac{3r^2}{l^2}\right) [1 - B(r)] \geq 0 \tag{37}$$

on the function $B(r)$. While using the conservation Eq. (14) plus constraint (28), condition (36) imposes the constraint

$$2(\mathcal{E} + \mathcal{P}_t) = -r\mathcal{E}' \geq 0 \tag{38}$$

on the function $\mathcal{E}(r)$.

Once again, to continue the process, we deliberately choose the energy density function of the additional source as the special monotonic function²

$$\mathcal{E}(r) = \frac{\alpha}{\kappa(\beta + r)^4}, \tag{39}$$

which satisfies³ both condition (34) and constraint (38), and has rapid asymptotic decay. In fact, considering Eq. (22) and choosing function (39), we have selected a special function for the geometric deformation $f(r)$ and in turn the function $B(r)$. In function (39), $r \neq -\beta$, where β is a constant parameter with length dimension that controls the behavior of $\mathcal{E}(r)$ at $r = 0$, i.e. it is necessary to avoid the central singularity.

² Also, this function is a reminder that the energy density of radiation is proportional to $1/r^4$.

³ Note that, the dimension of the deformation parameter is the square of length in the natural units.

We refer to the parameter β as a control parameter. In addition, the role of the deformation parameter in function (39) is consistent with Eq. (22). Meanwhile, substituting (39) into Eq. (38) gives

$$\mathcal{P}_t = \frac{r - \beta}{\beta + r} \mathcal{E}, \tag{40}$$

and in turn, by using relation (12) and constraint (28), the trace of the energy–momentum tensor $T_{\mu\nu}^{(X)}$ is obtained to be

$$T^{(X)} = -\frac{4\beta}{\beta + r} \mathcal{E}. \tag{41}$$

Thus, under the mentioned considerations, the energy–momentum tensor $T_{\mu\nu}^{(X)}$ depends only on a single function of the radial coordinate, its energy density function.

Now, by substituting function (39) into Eq. (33) and solving the differential equation for the function $B(r)$, we obtain

$$B(r) = \frac{\frac{\alpha\beta^2}{3(\beta+r)^3} + \frac{\alpha}{\beta+r} - \frac{\alpha\beta}{(\beta+r)^2} + r + \frac{r^3+c_1}{l^2}}{r(1 - 2M/r + r^2/l^2)}, \tag{42}$$

where c_1 is an integration constant. However, to have the background AdS-Schwarzschild solution (25) in the limit $\alpha \rightarrow 0$ (i.e., when $B(r) \xrightarrow{\alpha \rightarrow 0} 1$, and consistent with definition (32)), it is necessary to set⁴

$$c_1 = -2Ml^2. \tag{43}$$

Hence, the metric function reads

$$e^{\zeta(r)} B(r) = 1 - \frac{2M}{r} + \frac{r^2}{l^2} + \alpha \frac{\beta^2 + 3r^2 + 3\beta r}{3r(\beta + r)^3} \equiv F(r), \tag{44}$$

which preserves the asymptotic behavior in the form of the AdS solution. Moreover, the asymptotic behavior of the term resulting from the additional source is $1/r^2$, i.e. like a Maxwell field.

Therefore, the line element for the region outside a self-gravitating system filled with the energy–momentum tensor $T_{\mu\nu}^{(X)}$, while choosing the behavior of its energy density as function (39), is

$$ds^2 = -F(r) dt^2 + \frac{1}{F(r)} dr^2 + r^2(d\theta^2 + \sin^2\theta d\phi^2). \tag{45}$$

We refer to the black hole solution of this metric as a deformed AdS-Schwarzschild black hole, and in the next section, investigate its horizon structure and thermodynamics.

⁴ Note that, due to function (39), solution (42) with value (43) automatically satisfies constraint (37).

4 Structure of horizon and thermodynamics of deformed AdS-Schwarzschild black hole

First of all, the metric function (44) in the limit $\beta \rightarrow 0$ becomes the metric function corresponding to the well-known charged AdS black hole, i.e.

$$F(r)|_{\beta \rightarrow 0} = 1 - \frac{2M}{r} + \frac{r^2}{l^2} + \frac{\alpha}{r^2}. \tag{46}$$

Therefore, $\sqrt{\alpha}$ can be interpreted as the electric charge of black hole. In this particular case, the thermodynamic behavior of the black hole is reminiscent of that investigated in Refs. [7,41]. However, in these references, with the electric charge as a conserved charge of the theory, the possibility of variable electrostatic energy with an electric potential has been considered, while we consider the deformation parameter only as a free parameter.⁵ Moreover, we emphasize that in the case of $\beta = 0$, relation (41) indicates that the trace of the additional energy–momentum tensor is zero, and utilizing constraint (28) and relation (40) gives $\mathcal{P}_{\text{eff}} \equiv \frac{1}{3}(\mathcal{P}_r + \mathcal{P}_t + \mathcal{P}_t) = \frac{1}{3}\mathcal{E}$. These results plus the second footnote confirm that the additional energy–momentum tensor is the one of a Maxwell field and its solution is simply the electrically charged static AdS black hole.

On the other hand, we deliberately put the control parameter, i.e. β , by hand in function (39) so that $\beta \neq 0$ prevents the divergence of the energy density \mathcal{E} . Therefore, it is better to check the effect of the control parameter on the behavior of the metric function. For this purpose, we expand the metric function (44) around the zero of its argument to obtain

$$F(r)|_{r \rightarrow 0} = \frac{\frac{\alpha}{\beta} - 6M}{3r} + 1 + \frac{1}{3}r^2 \left(\frac{3}{l^2} - \frac{\alpha}{\beta^4} \right) + \mathcal{O}(r^3). \tag{47}$$

Hence, with the value of

$$\beta = \frac{\alpha}{6M}, \tag{48}$$

the metric function $F(r)$ has no singularity at $r = 0$. Further investigation of this particular case may lead to a regular black hole, however we leave this investigation to another work. That is, although relation (48) is necessary to avoid the divergence of the metric function, we do not limit our investigation to it in this work.

However, by the simple transformation $r \rightarrow \beta + r$, the control parameter is turned on. Hence, the energy–momentum tensor $T_{\mu\nu}^{(X)}$ no longer describes a pure Maxwell field and the corresponding metric is modified. Actually, we are interested to have the black hole solution of metric (45) in

⁵ Of course, the deformation parameter can also be considered as an additional hair that is not related to other charges, i.e. the mass, the electric charge and the angular-momentum.

the presence of non-vanishing β . For this purpose, the equation governing the radius of the event horizon r_h is determined by the larger root of equation

$$F(r_h) = 0, \tag{49}$$

which is a sixth order equation. Its solution is complicated and not useful for our purpose. Hence, instead of solving it analytically, we restrict ourselves to specifying its important consequences by resorting to its various corresponding diagrams in Fig. 1 with fixed values of its constants.

For each of the curves in this figure, the intersection of the metric function with the horizontal axis determines its corresponding event horizon radius. In this regard, this figure shows that the condition of having an event horizon limits the value of the deformation parameter to an upper bound, α_{\max} . In general, the value of α_{\max} depends on the values of other parameters, namely M, l and β . For instance, Fig. 1 indicates that when $M = 1, l = 1$ and $\beta = 1$, the radius of the event horizon decreases with increasing the value of α , until we obtain⁶ $\alpha_{\max} \approx 6$. In the continuation of this work, we pay attention to this limitation. In other words, we comply the value $0 < \alpha < \alpha_{\max}$ as a condition for having an event horizon for the deformed AdS-Schwarzschild black hole.

Alternatively, we have plotted the metric function $F(r)$, relation (44), with respect to r , while varying the control parameter β and fixing the other parameters including the deformation parameter α in Fig. 2. This figure shows that when $M = 1, l = 1$ and $\alpha = 4$, the radius of the event horizon increases with increasing the value of β . This effect is expected because the β parameter shifts the radial coordinate as mentioned earlier. In turn, increasing the radius of the event horizon affects the thermodynamic properties, and this indicates the influence of the control parameter on them.

To investigate the thermodynamic behavior of the obtained solution, while using Eq. (49), we first express the mass of the black hole in terms of the radius of the event horizon, i.e.

$$M = \frac{1}{6} \left[3r_h + \frac{3r_h^3}{l^2} + \alpha \frac{\beta^2 + 3r_h^2 + 3\beta r_h}{(\beta + r_h)^3} \right]. \tag{50}$$

Furthermore, the entropy of the deformed AdS-Schwarzschild black hole can be obtained from the Bekenstein–Hawking formula [2,42] as a quarter of the area of the event horizon, i.e.

$$S \equiv \frac{A_h}{4L_{\text{Pl}}^2} = \pi r_h^2, \tag{51}$$

where the Planck length L_{Pl} is considered in the natural units and the second equality is due to the static and spherical symmetry. Also, the definition of black hole pressure (density)

P in AdS space (in the natural units with a negative cosmological constant, see, e.g., Ref. [7]) is

$$P = \frac{3}{8\pi l^2}. \tag{52}$$

Then by obtaining r_h and l from relations (51) and (52), and substituting into relation (50), the mass of the deformed AdS-Schwarzschild black hole can also be expressed in terms of thermodynamic quantities S and P as

$$M = \frac{1}{6} \left[3\sqrt{\frac{S}{\pi}} + 8PS\sqrt{\frac{S}{\pi}} + \alpha \frac{\beta^2 + 3\frac{S}{\pi} + 3\beta\sqrt{\frac{S}{\pi}}}{\left(\beta + \sqrt{\frac{S}{\pi}}\right)^3} \right]. \tag{53}$$

Hence, for the deformed AdS-Schwarzschild black hole, we can write the (generalized) first law of black hole thermodynamics in the extended phase-space as⁷

$$dM = TdS + VdP, \tag{54}$$

where T and V are the Hawking temperature and the thermodynamic volume, respectively. Of course, in relation (54), the presence of VdP instead of PdV indicates that the mass M is the enthalpy of black hole instead of the internal energy.

Now, using relation (53), let us derive these thermodynamic quantities. In this regard, the temperature reads

$$T = \left(\frac{\partial M}{\partial S} \right)_P = \frac{1 + 8PS - \frac{\pi\alpha S}{(\sqrt{\pi}\beta + \sqrt{S})^4}}{4\sqrt{\pi S}}. \tag{55}$$

Of course, this relation can also be derived using the definition of the Hawking temperature in terms of the radius of the event horizon, i.e.

$$T \equiv \frac{1}{4\pi} F'(r)|_{r=r_h} = \frac{1 + r_h^2 \left[\frac{3}{l^2} - \frac{\alpha}{(\beta + r_h)^4} \right]}{4\pi r_h}, \tag{56}$$

where we have substituted M from relation (53). Then, taking r_h and l from relations (51) and (52), and substituting into relation (56), it reads the same as relation (55) as expected. Also, the thermodynamic volume is [43,44]

$$V = \left(\frac{\partial M}{\partial P} \right)_S = \frac{4S^{3/2}}{3\sqrt{\pi}} \tag{57}$$

that, in terms of the radius of the event horizon, obviously reads

$$V = \frac{4}{3}\pi r_h^3. \tag{58}$$

⁷ Note that, in this law, we do not consider the deformation parameter as a possibility of variable electrostatic energy, see, e.g., Ref. [38]. Nevertheless, if one puts a term like $+\Phi d\alpha$ in the right hand of relation (54), due to partial derivatives, relations (55), (57) and (61) will not change, and by definition (59), relation (60) will not change either.

⁶ However, using Eq. (49) with these mentioned values gives $\alpha = 3(2 - r_h - r_h^2)(1 + r_h^3)/(1 + 3r_h + 3r_h^2)$ that yields $\alpha \xrightarrow{r_h \rightarrow 0} 6$.

Fig. 1 Using relation (44), the figure schematically (i.e., scale-free) illustrates the behavior of the function $F(r)$ with respect to r for fixed values of $M = 1, l = 1$ and $\beta = 1$, and different chosen values of α . As α increases, the radius of the event horizon decreases, until $\alpha_{\max} \approx 6$

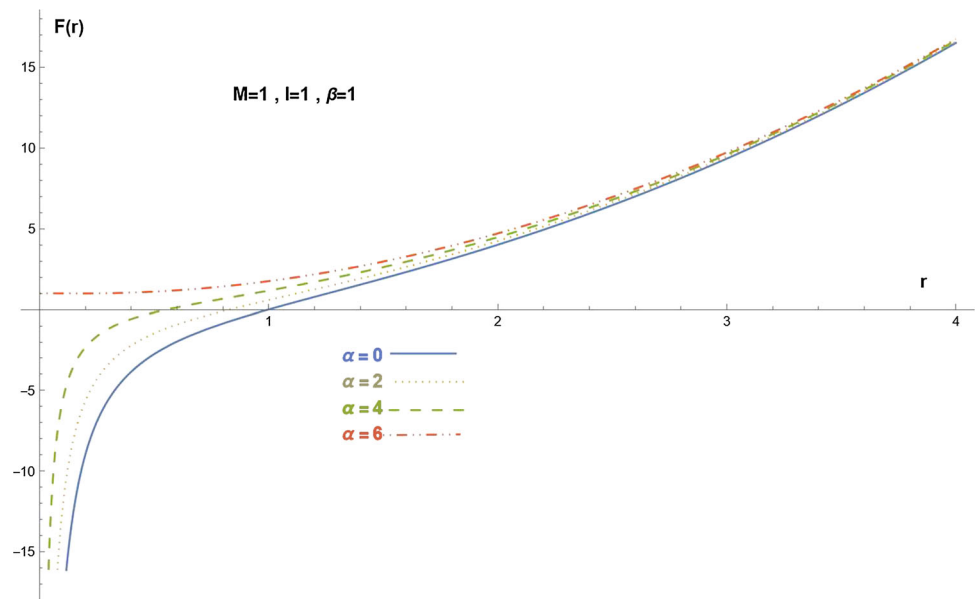
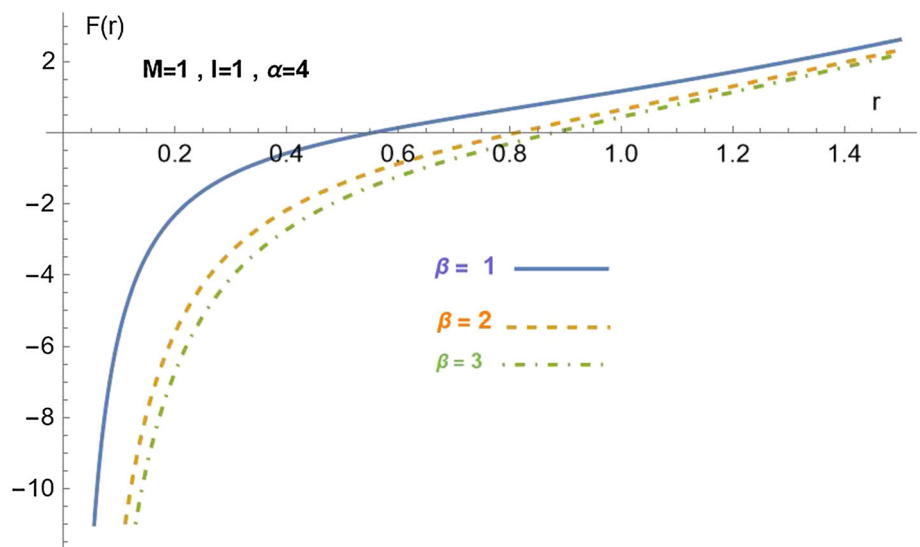


Fig. 2 Using relation (44), the figure schematically (i.e., scale-free) illustrates the behavior of the function $F(r)$ with respect to r for fixed values of $M = 1, l = 1$ and $\alpha = 4$, and different chosen values of β . As β increases, the radius of the event horizon increases



To continue investigation of the thermodynamic behavior of the deformed AdS-Schwarzschild black black hole, we apply the thermodynamic machinery suggested in Ref. [7]. We assume that the black hole occurs in a canonical ensemble. We also assume that each related extended phase-space contains a fixed value of the deformation parameter. In this case, the Gibbs free energy is⁸

$$G \equiv M - TS, \tag{59}$$

which in terms of the radius of the event horizon becomes

$$G = \frac{r_h}{4} - \frac{r_h^3}{4l^2} + \alpha \frac{9r_h^3 + 12\beta r_h^2 + 8\beta^2 r_h + 2\beta^3}{12(\beta + r_h)^4}. \tag{60}$$

⁸ We do not consider the deformation parameter in this relation either.

In this regard, it is known that the condition of better thermal equilibrium globally corresponds with more negative values of the Gibbs free energy. Also, the criterion of the phase transition is related to the vanishing Gibbs free energy of the black hole.

Another useful quantity in the thermodynamic study of a black hole is the specific heat capacity at constant pressure, C_P , which determines the local thermodynamic stability of the black hole. In the case at hand, it is

$$C_P \equiv T \left(\frac{\partial S}{\partial T} \right)_P = 2\pi \frac{1 + r_h^2 \left[\frac{3}{l^2} - \frac{\alpha}{(\beta + r_h)^4} \right]}{\frac{3}{l^2} - \frac{1}{r_h^2} - \frac{\alpha}{(\beta + r_h)^4} + \frac{4\alpha r_h}{(\beta + r_h)^5}}, \tag{61}$$

where we have used the chain rule and relation (56). However, the local thermodynamic stability corresponds to positive C_P values.

On the other hand, among the various black hole phase transitions, one of the most significant is the Hawking–Page phase transition [13]. This is a study of the thermodynamics between an AdS-Schwarzschild black hole and the thermal AdS space. In this respect, we consider the constant values of $\beta = 1$ and⁹ $l = 1$ and choose several constant values of the deformation parameter within its allowed range to investigate its effects on the stability of the black hole and particularly on the Hawking–Page phase transition.

First, let us investigate the thermodynamic stability of the black hole locally through the behavior of the specific heat capacity at constant pressure. In this regard, Fig. 3 indicates the behavior of the C_P function with respect to the radius of the event horizon for several values of the deformation parameter in its allowed range. The resulting curves contain a discontinuity at a certain horizon radius, such that for the chosen values it is approximately in the range of $0.55 < r_h < 0.6$. Moreover, the black holes with horizon radii located in the region of negative C_P values are thermodynamically unstable, and a minimum value of horizon radius is required for a black hole to have local thermodynamic equilibrium. However, as the deformation parameter increases, such minimum required radius decreases. Figure 3 also shows that black holes in the $C_P < 0$ region have small horizon radii (which we refer to as small black holes (SBHs)) and transform into other thermodynamically allowed states. However, black holes with larger horizon radii in the $C_P > 0$ region (which we refer to as large black holes (LBHs)) have a clear local thermodynamic stability. Hence, LBHs are thermodynamically preferred over SBHs. In addition, according to this figure, as α increases, the horizon radius of locally stable black holes decreases. Furthermore, in the region of LBHs, for all curves, as the horizon radius increases, the corresponding value of C_P first decreases to a minimum and then increases. To scrutinize the thermodynamic behavior of black holes globally, we investigate the behavior of the Gibbs free energy function.

In this regard, first we have depicted the G function versus r_h with fixed values of $\beta = 1$ and $l = 1$, and different chosen values of α in Fig. 4. It is clear that the global thermodynamic equilibrium is better achieved with less negative values of the G function. Here, as an important aspect, this figure illustrates that LBHs have less negative values of the G function. Hence, Fig. 4 confirms that in addition to local thermodynamic stability, this group of black holes also has global thermodynamic stability, while SBHs do not. Thus once again, LBHs are thermodynamically preferred over SBHs. This figure also shows that the function G is first ascending and then descending for all allowed values of the deformation parameter. However, as the deformation

parameter increases, these maximum values of the G function and also the horizon radius of the phase transition (wherein $G = 0$) increase. Nevertheless, increasing the deformation parameter causes the thermodynamic stability of a black hole to be disturbed compared to its previous position. Also, each maximum point of the G function represents a horizon radius and a temperature. However, to better realize the phase transition and the global thermodynamic stability of black holes, we probe the behavior of the G function versus the horizon temperature in the following figure. Although it is better and instructive to first plot the temperature versus the radius of the event horizon.

In this respect, Fig. 5 shows the behavior of the temperature of horizon with respect to r_h for fixed values of $\beta = 1$ and $l = 1$, and different chosen values of α . This figure indicates that as r_h increases, the temperature of horizon first decreases and then increases for all values of α . The minimum temperature in this figure exactly corresponds to the maximum Gibbs function in Fig. 4. In general, the changing behavior of the temperature function is in accord with the behavior of the G function.

Now, employing relations (56) and (60), Fig. 6 shows the behavior of the Gibbs function with respect to the horizon temperature for fixed values of $\beta = 1$ and $l = 1$, and different chosen values of the deformation parameter. The cusp of each curve in this figure represents the maximum of the G function (as shown in Fig. 4) and the minimum temperature (as shown in Fig. 5). At temperatures below the minimum temperature, there are no black holes. Figure 6 indicates that as the temperature increases from its minimum, there are two branches of black holes. In both branches the G function decreases, which is in accordance with Fig. 4. The right/upper branches contain SBHs with $C_P < 0$, while the left/lower branches have $C_P > 0$ and include black holes with intermediate horizon radii (which we refer to as intermediate black holes (IBHs)) with positive values of the G function, the intersection of curves with the horizontal axis (the phase transition with $G = 0$), and LBHs with negative values of the G function.

Since thermodynamically, smaller (and even negative) values of the G function are preferred, there are actually two global thermodynamically stable phases. The first phase in which $G = 0$ represents the immersion environment of black holes and includes the thermal radiation (the thermal bath filled with the cosmological constant). This region is preferred with respect to IBHs. The second phase belongs to LBHs, which indicate more stability and thermodynamic preference. The proximity of the phase transition between the thermal radiation medium and the deformed AdS-Schwarzschild LBHs is known as the Hawking–Page phase transition. The intersection of the curves with the horizontal axis shows the temperature of the first-order Hawking–Page phase transition. Figure 6 also illustrates that as the

⁹ Actually, considering relation (52), we investigate the thermodynamic behaviors at constant pressure.

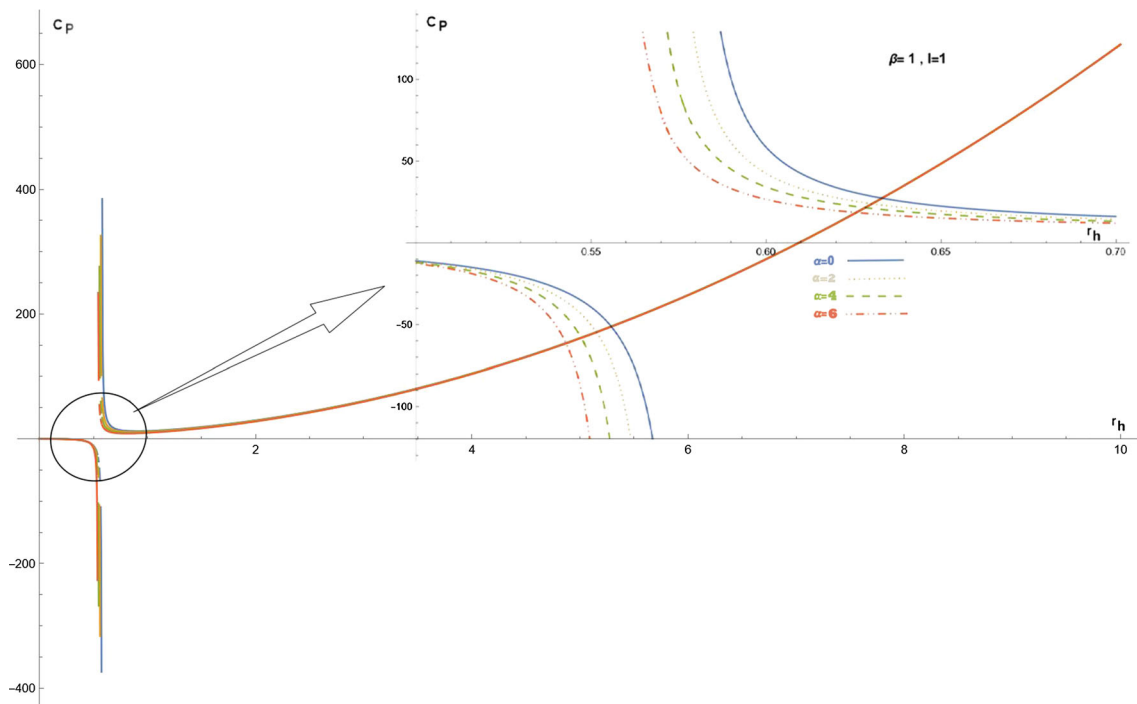
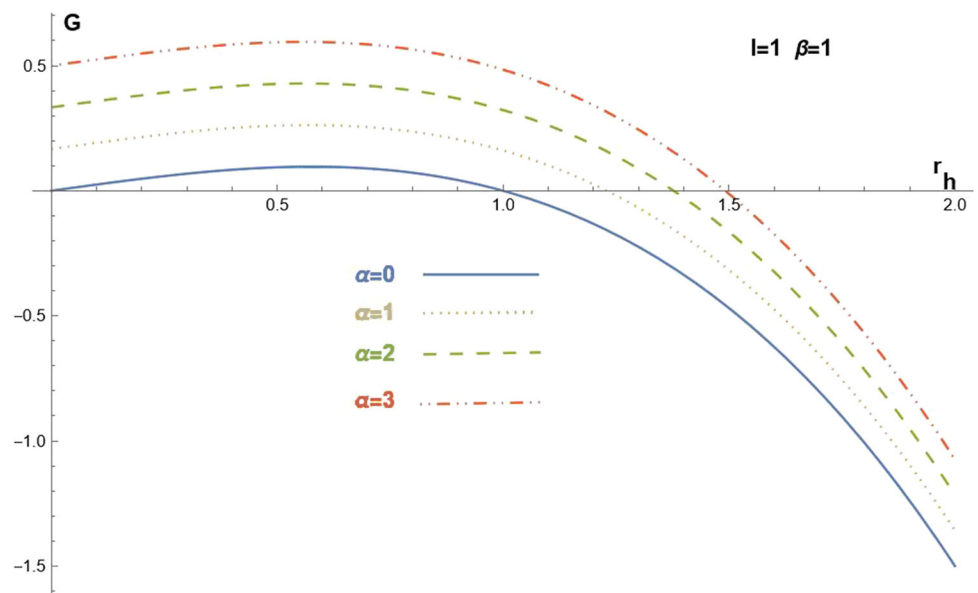


Fig. 3 Using relation (61), the figure schematically (i.e., scale-free) illustrates the behavior of the C_P function with respect to r_h for fixed values of $\beta = 1$ and $l = 1$, and different chosen values of α . In the $C_P < 0$ region, the black holes do not have local thermodynamic equilibrium.

In the $C_P > 0$ region, as α increases, the black holes with smaller horizon radii have local thermodynamic equilibrium. Also, in this region for all curves, as r_h increases, the corresponding value of C_P first decreases to a minimum and then increases

Fig. 4 Using relation (60), the figure schematically (i.e., scale-free) illustrates the behavior of the function G with respect to r_h for fixed values of $\beta = 1$ and $l = 1$, and different chosen values of α . The intersection points of the curves with the horizontal axis (i.e., $G = 0$) indicate the horizon radius of the phase transition. As α increases, the r_h of the phase transition and the maximum value of the G function also increase. More interestingly, in the $G < 0$ region, black holes with larger r_h have less negative G function



deformation parameter increases, the G function and especially its maximum increases (consistent with Fig. 4), the minimum temperature decreases (consistent with Fig. 5) while the temperature of the Hawking–Page phase transition increases.

5 Conclusions

Initially, we considered the Einstein–Hilbert action with the presence of the cosmological constant and a standard matter source plus any additional gravitational source. The aim of this work is to find the black hole solution(s) for such an action and to search for the corresponding thermodynamic behaviors. To proceed, we have employed the GD

Fig. 5 Using relation (56), the figure schematically (i.e., scale-free) illustrates the behavior of the temperature of horizon with respect to r_h for fixed values of $\beta = 1$ and $l = 1$, and different chosen values of α . As r_h increases, the horizon temperature first decreases to a minimum and then increases

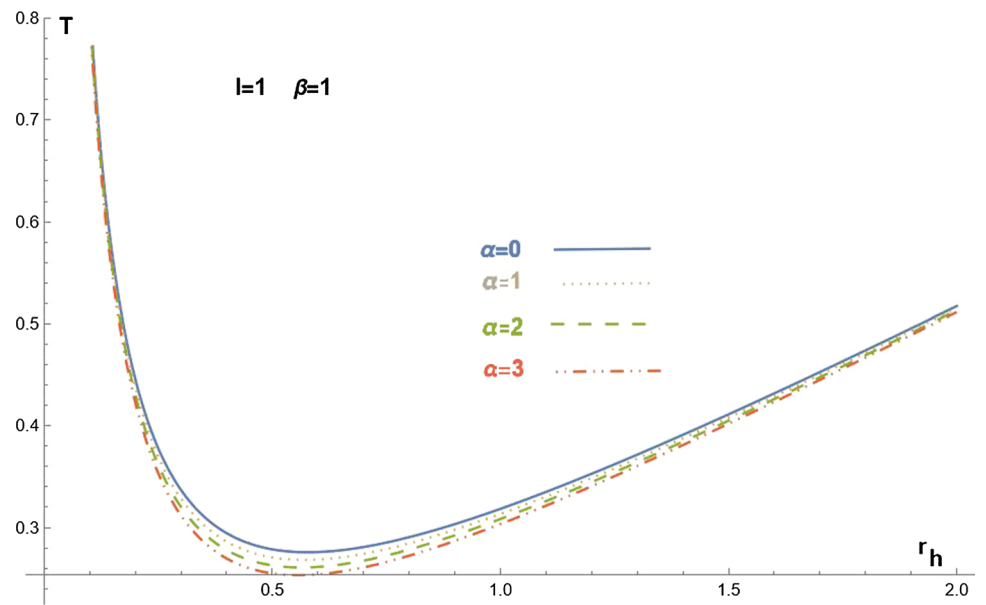
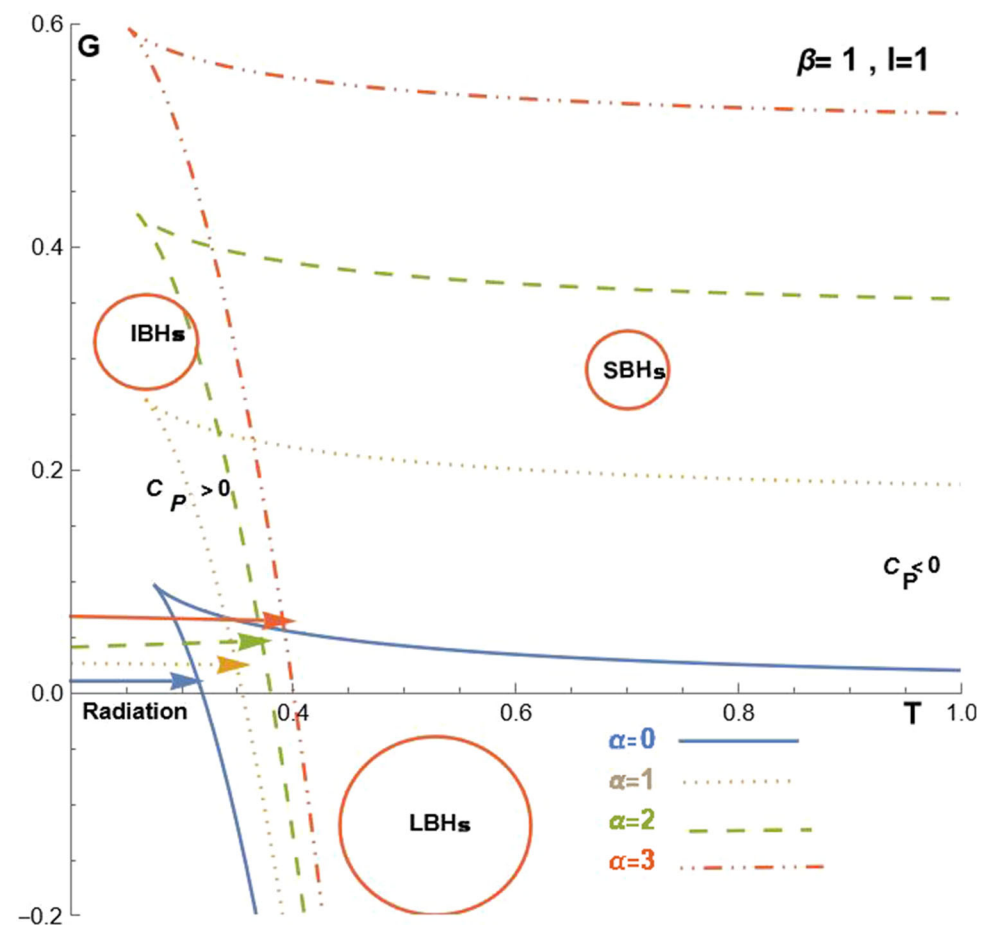


Fig. 6 The figure schematically (i.e., scale-free) illustrates the behavior of the G function with respect to the horizon temperature for fixed values of $\beta = 1$ and $l = 1$, and different chosen values of α . A deformed AdS-Schwarzschild black hole, like a Schwarzschild black hole, exhibits a phase transition with a thermal radiation medium. The region of the thermal radiation is indicated by an arrow for each curve, and the end of each arrow indicates the temperature of the first-order Hawking–Page phase transition



method, which serves as a useful tool for searching solutions to the gravitational equations. Then, we have taken the background as the AdS-Schwarzschild vacuum solution, and have looked for the static spherically symmetric solution(s) when the additional source is also present. By implementing the GD method, we have used two geometric deformation functions to alter the radial and temporal components of the background metric. Meanwhile, in process of this method, there is a common positive parameter that can adjust the strength of the effects on these components simultaneously, and we refer to it as a deformation parameter. When this parameter vanishes, the background solution is recovered. Through the GD method, the field equations are separated into two decoupled sets of equations for each source, although they remain gravitationally connected.

In continuation, after solving the set of equations for the background, five unknowns remain in the three equations corresponding to the additional source. Hence, to solve this set, we imposed two constraints. Actually, we have assumed that the additional source obeys the weak energy condition, and we have also deliberately chosen its energy density function to be a special monotonic function proportional to the inverse of the distance to the fourth power. Also for consistency, this function is proportional to the deformation parameter and includes a control parameter to prevent it from diverging at the center. Actually, in the absence of the control parameter, we showed that the additional energy–momentum tensor is the one of a Maxwell field. Moreover, to have black holes with a well-defined event horizon structure, we have imposed the Kerr–Schild condition that the radial and temporal components of the solution to be inverses of each other regardless of their signs in the signature. We refer to the obtained solution as a deformed AdS-Schwarzschild black hole. The solution found, although complicated, turns out to be analytical and with quite interesting features. Then, the focus of the work has been to investigate the horizon structure, the thermodynamics of the solution and the Hawking–Page phase transition mainly by varying the deformation parameter. However, within the work (including figures), we considered several values of the deformation parameter with fixed values of other constants (hence, actually at constant pressure).

Since we intended to consider the black hole solution, we first plotted the metric function versus the distance. For each of the curves in this figure, the intersection of the metric function with the horizontal axis specifies that there is an event horizon radius. However, the figure shows that the condition of having an event horizon limits the value of the deformation parameter to an upper bound, as we have also shown through the corresponding derivation. Hence, we confined the investigation to vary the deformation parameter up to its upper bound value.

Next, we assumed that the black hole occurs in a canonical ensemble and wrote the first law of black hole thermody-

namics in the extended phase-space and then derived various thermodynamic quantities as a function of the event horizon radius. We also assumed that each related extended phase-space contains a fixed value of the deformation parameter as a free parameter and not a thermodynamic quantity. Thereafter, to determine the thermodynamic stability of the black hole locally, we plotted the obtained heat capacity at constant pressure versus the radius of the event horizon. The figure shows that a discontinuity occurs between the negative and positive values of the heat capacity at constant pressure for all its curves. The negative region contains SBHs that are locally thermodynamically unstable. Whereas, the positive region contains LBHs that are locally thermodynamically stable. In other words, for a black hole to have local thermodynamic equilibrium, a minimum value of horizon radius is required, and as the deformation parameter increases, this minimum required radius decreases. In addition, in the region of LBHs, for all curves, as the horizon radius increases, the corresponding value of C_p first decreases to a minimum and then increases, while as the deformation parameter increases, the horizon radius of locally stable black holes decreases.

Furthermore, to determine the thermodynamic stability of the black hole globally, we plotted the obtained Gibbs free energy versus the radius of the event horizon. This figure shows that the Gibbs function starts from the region of positive values, and with the increase of the horizon radius, it first increases to a maximum and then decreases to more negative values after crossing the horizontal axis (i.e., the phase transition point). The figure also illustrates that LBHs have less negative values of the Gibbs free energy. Hence, in addition to local thermodynamic stability, this group of black holes also has global thermodynamic stability and is thermodynamically preferred over SBHs. Moreover, with the increase of the deformation parameter, the maximum values of the Gibbs function and the horizon radius of the phase transition increase. Nevertheless, increasing the deformation parameter causes the thermodynamic stability of a black hole to be disturbed compared to its previous position.

Then, to better realize the phase transition and global thermodynamic stability of black holes, we plotted the temperature versus the event horizon radius and the Gibbs free energy versus the horizon temperature. The figures indicate that there is a minimum temperature that exactly corresponds to the maximum of the Gibbs function. As the deformation parameter increases, the minimum temperature decreases and no black hole exists below this minimum temperature. The second figure illustrates that SBHs are in one branch of the curves, and in the other branch are IBHs, the phase transition point (i.e., thermal radiation) and LBHs. The proximity of the phase transition between the thermal radiation medium and the deformed AdS-Schwarzschild LBHs is known as the Hawking–Page phase transition. As the deformation param-

eter increases, the temperature of the first-order Hawking–Page phase transition increases.

In the special case of vanishing the deformation parameter, the obtained thermodynamic behavior of the black hole is consistent with that stated in Ref. [7]. Also, we showed that in the special case of vanishing the control parameter, the obtained metric function corresponds to the charged AdS black hole, which was investigated in Refs. [7,41] with the square of the deformation parameter as the role of electric charge. In addition, we showed that increasing the control parameter increases the radius of the event horizon, which in turn affects the thermodynamic properties. Furthermore, we indicated that for a certain non-zero value of the control parameter, the obtained metric function has no singularity at the center. Further investigation of this particular case may lead to a regular black hole, however we leave these investigations to another work.

Acknowledgements The authors thank the Research Council of Shahid Beheshti University.

Data Availability Statement This manuscript has no associated data or the data will not be deposited. [Authors' comment: This work is a theoretical study and has no experimental data.]

Open Access This article is licensed under a Creative Commons Attribution 4.0 International License, which permits use, sharing, adaptation, distribution and reproduction in any medium or format, as long as you give appropriate credit to the original author(s) and the source, provide a link to the Creative Commons licence, and indicate if changes were made. The images or other third party material in this article are included in the article's Creative Commons licence, unless indicated otherwise in a credit line to the material. If material is not included in the article's Creative Commons licence and your intended use is not permitted by statutory regulation or exceeds the permitted use, you will need to obtain permission directly from the copyright holder. To view a copy of this licence, visit <http://creativecommons.org/licenses/by/4.0/>.

Funded by SCOAP³. SCOAP³ supports the goals of the International Year of Basic Sciences for Sustainable Development.

References

1. S.W. Hawking, Black holes in general relativity. *Commun. Math. Phys.* **25**, 152 (1972)
2. J.D. Bekenstein, Black holes and entropy. *Phys. Rev. D* **7**, 2333 (1973)
3. J.M. Bardeen, B. Carter, S.W. Hawking, The four laws of black hole mechanics. *Commun. Math. Phys.* **31**, 161 (1973)
4. S.W. Hawking, Particle creation by black holes. *Commun. Math. Phys.* **43**, 199 (1975)
5. R.M. Wald, The thermodynamics of black holes. *Living Rev. Relativ.* **4**, 6 (2001)
6. S. Carlip, Black hole thermodynamics. *Int. J. Mod. Phys. D* **23**, 1430023 (2014)
7. D. Kubizňák, R.B. Mann, M. Teo, Black hole chemistry: thermodynamics with lambda. *Class. Quantum Gravity* **34**, 063001 (2017)
8. C. Tetelboim, The cosmological constant as a thermodynamic black hole parameter. *Phys. Lett. B* **158**, 293 (1985)
9. J.D. Brown, C. Tetelboim, Neutralization of the cosmological constant by membrane creation. *Nucl. Phys. B* **297**, 787 (1988)
10. N. Farhangkhan, Z. Dayyani, Extended phase space thermodynamics for third-order Lovelock black holes with non-maximally symmetric horizons. *Phys. Rev. D* **104**, 024068 (2021)
11. K. Bhattacharya, Extended phase space thermodynamics of black holes: a study in Einstein's gravity and beyond. *Nucl. Phys. B* **989**, 116130 (2023)
12. D. Kastor, S. Ray, J. Traschen, Entropy and the mechanics of AdS black holes. *Class. Quantum Gravity* **26**, 195011 (2009)
13. S.W. Hawking, D.N. Page, Thermodynamics of black holes in anti-de Sitter space. *Commun. Math. Phys.* **87**, 577 (1983)
14. E. Witten, Anti-de Sitter space, thermal phase transition and confinement in gauge theory. *Adv. Theor. Math. Phys.* **2**, 505 (1998)
15. D. Kastor, S. Ray, J. Traschen, Smarr formula and an extended first law for Lovelock gravity. *Class. Quantum Gravity* **27**, 235014 (2010)
16. D.C. Zou, S.J. Zhang, B. Wang, Critical behavior of Born–Infeld AdS black hole in the extended phase space thermodynamics. *Phys. Rev. D* **89**, 044002 (2014)
17. N. Altamirano, D. Kubiznak, R.B. Mann, Reentrant phase transitions in rotating AdS black holes. *Phys. Rev. D* **88**, 101502 (2013)
18. R.-G. Cai, L.-M. Cao, L. Li, R.-Q. Yang, P-V criticality in the extended phase space of Gauss–Bonnet black holes in AdS space. *J. High Energy Phys.* **2013**, 5 (2013)
19. N. Altamirano, D. Kubiznak, R.B. Mann, Z. Sherkatghanad, Kerr–AdS analogue of triple point and solid/liquid/gas phase transition. *Class. Quantum Gravity* **31**, 042001 (2014)
20. B.P. Dolan, A. Kostouki, D. Kubiznak, R.B. Mann, Isolated critical point from Lovelock gravity. *Class. Quantum Gravity* **31**, 242001 (2014)
21. H. Xu, W. Xu, L. Zhao, Extended phase space thermodynamics for third order Lovelock black holes in diverse dimensions. *Eur. Phys. J. C* **74**, 3074 (2014)
22. D.C. Zou, R. Yue, M. Zhang, Reentrant phase transitions of higher-dimensional AdS black holes in dRGT massive gravity. *Eur. Phys. J. C* **77**, 256 (2017)
23. J. Ovalle, Decoupling gravitational sources in general relativity: from perfect to anisotropic fluids. *Phys. Rev. D* **95**, 104019 (2017)
24. J. Ovalle, Decoupling gravitational sources in general relativity: the extended case. *Phys. Lett. B* **788**, 213 (2019)
25. J. Ovalle, R. Casadio, A. Giusti, Regular hairy black holes through Minkowski deformation. *Phys. Lett. B* **844**, 138085 (2023)
26. J. Ovalle, Searching exact solutions for compact stars in brane world: a conjecture. *Mod. Phys. Lett. A* **23**, 3247 (2008)
27. J. Ovalle, F. Linares, Tolman IV solution in the Randall–Sundrum braneworld. *Phys. Rev. D* **88**, 104026 (2013)
28. R. Casadio, J. Ovalle, R. da Rocha, The minimal geometric deformation approach extended. *Class. Quantum Gravity* **32**, 215020 (2015)
29. A. Fernandes-Silva, A.J. Ferreira-Martins, R. da Rocha, The extended minimal geometric deformation of SU(N) dark glueball condensates. *Eur. Phys. J. C* **78**, 631 (2018)
30. J. Ovalle, R. Casadio, R. da Rocha, A. Sotomayor, Z. Stuchlik, Black holes by gravitational decoupling. *Eur. Phys. J. C* **78**, 960 (2018)
31. A'. Rinc'on, L. Gabbanelli, E. Contreras and F. Tello–Ortiz, Minimal geometric deformation in a Reissner–Nordström background. *Eur. Phys. J. C* **79**, 873 (2019)
32. A'. Rinc'on, E. Contreras, F. Tello–Ortiz, P. Bargueño and G. Abellán, Anisotropic 2 + 1 dimensional black holes by gravitational decoupling. *Eur. Phys. J. C* **80**, 490 (2020)
33. R. da Rocha, A.A. Tomaz, MGD-decoupled black holes, anisotropic fluids and holographic entanglement entropy. *Eur. Phys. J. C* **80**, 857 (2020)

34. J. Ovalle, R. Casadio, E. Contreras, A. Sotomayor, Hairy black holes by gravitational decoupling. *Phys. Dark Univ.* **31**, 100744 (2021)
35. E. Contreras, J. Ovalle, R. Casadio, Gravitational decoupling for axially symmetric systems and rotating black holes. *Phys. Rev. D* **103**, 044020 (2021)
36. S. Mahapatra, I. Banerjee, Rotating hairy black holes and thermodynamics from gravitational decoupling. *Phys. Dark Univ.* **39**, 101172 (2023)
37. R. Avalos, E. Contreras, Quasi normal modes of hairy black holes at higher-order WKB approach. *Eur. Phys. J. C* **83**, 155 (2023)
38. R. Avalos, P. Bargeño, E. Contreras, A static and spherically symmetric hairy black hole in the framework of the gravitational decoupling. *Fortsch. Phys.* **71**, 2200171 (2023)
39. Y. Meng, X.-M. Kuang, X.-J. Wang, B. Wang, J.-P. Wu, Images from disk and spherical accretions of hairy Schwarzschild black holes. *Phys. Rev. D* **108**, 064013 (2023)
40. F. Tello-Ortiz, A. Rincón, A. Alvarez and S. Ray, Gravitationally decoupled non-Schwarzschild black holes and wormhole “space-times”, *Eur. Phys. J. C* **83**, 796 (2023)
41. H. Abdusattar, Stability and Hawking-Page-like phase transition of phantom AdS black holes. *Eur. Phys. J. C* **83**, 614 (2023)
42. G. Gibbons, S. Hawking, Cosmological event horizons, thermodynamics, and particle creation. *Phys. Rev. D* **15**, 2738 (1977)
43. B.P. Dolan, The cosmological constant and the black hole equation of state. *Class. Quantum Gravity* **28**, 125020 (2011)
44. M. Cvetič, G.W. Gibbons, D. Kubizňák, C.N. Pope, Black hole enthalpy and an entropy inequality for the thermodynamic volume. *Phys. Rev. D* **84**, 024037 (2011)